Effects of pressure on the electric field gradient in USn_3

2005 J. Phys.: Condens. Matter 17 2407

(http://iopscience.iop.org/0953-8984/17/15/012)

INSTITUTE OF PHYSICS PUBLISHING JOURNAL OF PHYSICS: CONDENSED MATTER

J. Phys.: Condens. Matter **17** (2005) 2407–2418 doi:10.1088/0953-8984/17/15/012

Effects of pressure on the electric field gradient in USn_3

Z Nourbakhsh[1], H Akbarzadeh[2] and A Pourghazi[1,3]

[1] Physics Department, University of Isfahan, Isfahan, Iran
[2] Physics Department, Isfahan University of Technology, Isfahan, Iran

E-mail: apour@sci.ui.ac.ir

Received 20 December 2004, in final form 17 February 2005
Published 1 April 2005
Online at stacks.iop.org/JPhysCM/17/2407

Abstract

The structural and electronic properties of USn_3 have been calculated in the presence and in the absence of spin–orbit interaction using density functional theory by the Wien2k package. Both the energy band calculation and the density of states curves indicate that spin–orbit interaction has a considerable effect and cannot be ignored. Thus the calculation of the electric field gradient (EFG) as a function of pressure has been performed in the presence of spin–orbit coupling. The contributions of different orbitals to the EFG show that the strongest anisotropy in the charge distribution is due to the electrons in p orbitals.

1. Introduction

USn_3 belongs to a series of compounds labelled UM_3 (M being an element of group III or IV of the periodic table). In these compounds uranium 5f electrons may have the usual itinerant character in the compound (as in USi_3) or exhibit a more narrow-band-like behaviour as M moves down from Si to Pb in the periodic table [1]. These compounds have cubic Cu_3Au-type structure, where the Au atoms are on the vertices and the Cu atoms on the face centres of the unit cell.

The electronic and magnetic properties of these compounds range from Pauli paramagnetism, with enhanced γ values of about 40 mJ mol^{-1} K^{-2} (M = Al, Si, Ge), to local moment behaviour (M = Tl, Pb) with itinerant antiferromagnetism (M = Ga, In). USn_3 is near the boundary between itinerant and localized f electrons [2]. The electronic and magnetic properties of USn_3 including magnetic excitations [3], electronic properties [4], electronic heat capacity [5] and quantum oscillations in high magnetic fields [4] have been investigated through theoretical and experimental methods.

[3] Author to whom any correspondence should be addressed.

0953-8984/05/152407+12$30.00

In this work we have calculated the electric field gradient around the Sn nucleus in the presence of spin–orbit coupling for the USn_3 compound. We have also investigated the effect of pressure on the electric field gradient and on the anisotropy of the charge distribution close to the Sn nucleus and studied the structural and electronic properties of this compound.

2. Calculation methods

The calculated results in this paper were obtained using the highly accurate full potential linearized augmented plane wave plus local orbital (APW + LO) method as implemented in the Wien2k code [6]. In this procedure, each unit cell is divided into non-overlapping muffin-tin (MT) spheres of radii R_{MT} and an interstitial region, where the Kohn–Sham (KS) wavefunctions are expressed in spherical harmonics within the MT spheres and in plane waves in the interstitial region. The charge density and potential are expanded in lattice harmonics inside muffin-tin spheres and as a Fourier series in the remaining space. In our work the maximum quantum number l for atomic wavefunctions inside the sphere was confined to $l_{max} = 10$. The wavevector cut-off for the plane wave expansion of the wavefunction in the interstitial region was $K_{max} = \frac{7}{R_{MT}}$ where R_{MT} is the smallest muffin-tin radius in the unit cell. The charge density and potential were Fourier expanded in the interstitial region up to $G_{max} = 16$. For U, the muffin-tin radius was chosen as $R_U = 2.7$ au, while for Sn a radius of $R_{Sn} = 2.4$ au was used. A mesh of 120 k-points was generated in the irreducible wedge of the Brillouin zone. For the exchange–correlation potential we used the local density approximation (LDA) with and without the generalized gradient correction (GGA) based on the Perdew, Burke and Ernzerhof [7] scheme. Our calculations for core electrons were performed fully relativistically, while the valence electrons were treated in both scalar and fully relativistic fashions. Applying spin–orbit coupling for the valence electrons in the Wien2k code is performed by a second-variational treatment [8, 9]. In this scheme the spin–orbit term is set up in a subspace spanned by the scalar relativistic solution with about twice the number of the occupied orbitals but much less than the full basis.

By performing the total energy calculations in actinide systems Nordstrom *et al* [10] found that the description of the 6p states using the scalar relativistic basis is not reliable. Kunes *et al* [11] recalculated the electronic structure of fcc Th by including $p_{1/2}$ local orbitals (LO) in the basis set of the second-variation step for the low lying 6p semicore states. Their results confirm that the addition of these extra LOs for semicore states is necessary for unambiguously calculating the equilibrium volumes. Furthermore these extra LOs remove to a large extent the strong dependence of the total energy on the MT radius and improve the total energy convergence by producing a reduction in the plane wave energy cut-off. For total energy calculation of USn_3 we followed Kunes *et al* [11] and included $p_{1/2}$ local orbitals in the basis set. We found that the extra LOs reduce the cut-off energy for USn_3, but some fluctuations were observed in the electric field gradient (EFG) calculated at this reduced cut-off energy. Thus we performed EFG calculations without these extra LOs.

3. Results and discussion

3.1. The effect of spin–orbit interaction on the structural and electronic properties of USn_3

In order to investigate the effect of spin–orbit coupling on the structural properties of USn_3, the total energy per unit cell as a function of volume is calculated. In this calculation we used the experimental lattice parameter [4, 12] as the starting point and fitted the results with a Murnaghan equation of state [13]. The total energy–volume curves are compared in figure 1

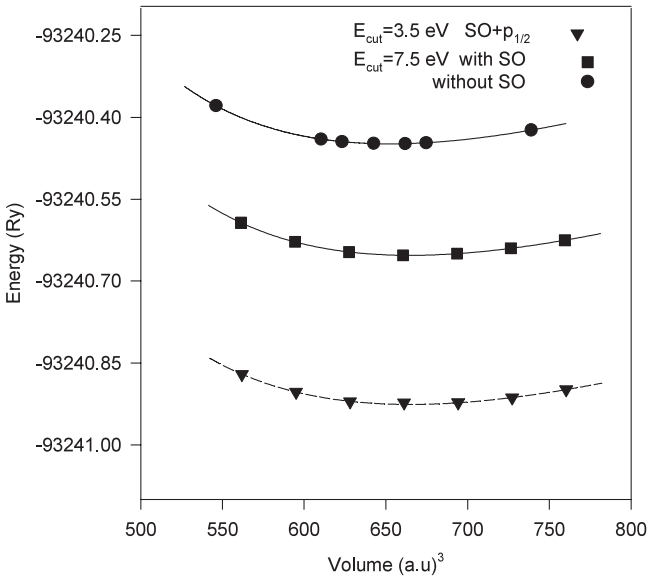

Figure 1. Total energy as a function of unit cell volume in the absence of spin–orbit coupling, and in the presence of spin–orbit coupling with and without the $p_{1/2}$ local orbital.

Table 1. Structural parameters of USn_3.

	GGA	GGA + SO	GGA + SO + $p_{1/2}$	Experiment
Lattice parameter (Å)	4.588	4.613	4.616	4.610 [4] 4.609 [12]
Bulk modulus (GPa)	82.10	80.30	73.85	83 [14]
Pressure derivative of bulk modulus	5.24	4.37	4.61	—

Table 2. The linear coefficient of the electronic specific heat and EFG at the Sn site of USn_3.

	GGA	GGA + SO	LDA	LDA + SO	Experiment	Other works
γ (mJ mol^{-1} K^{-2})	11.97	26.47	16.04	28.85	171 [12]	16.96 [15]
λ	13.20	5.42	9.59	4.89	—	9.0 [15]
EFG at Sn site (10^{21} V m^{-2})	21.45	21.08	22.26	21.88	—	—

in the absence of SO, in the presence of this term and in the presence of SO + LOs. The corresponding equilibrium lattice parameters, bulk moduli and their pressure derivatives are compared with experiment in table 1. The equilibrium lattice parameter calculated in the presence of spin–orbit coupling is in better agreement with the experiment but the addition of $p_{1/2}$ local orbitals has no significant effect on the equilibrium volume. The SO coupling term reduces the total energy and increases the equilibrium lattice parameter. We have found that the bulk modulus calculated in the absence of spin–orbit coupling is in good agreement with the experiment [14] while the SO term with and without local orbitals reduces it.

Furthermore by using the calculated density of states at the Fermi level, $D(E_f)$, we obtained the linear coefficient γ of the electronic specific heat. The results are compared with other theoretical and experimental results [12, 15] in table 2, which shows that all the theoretical

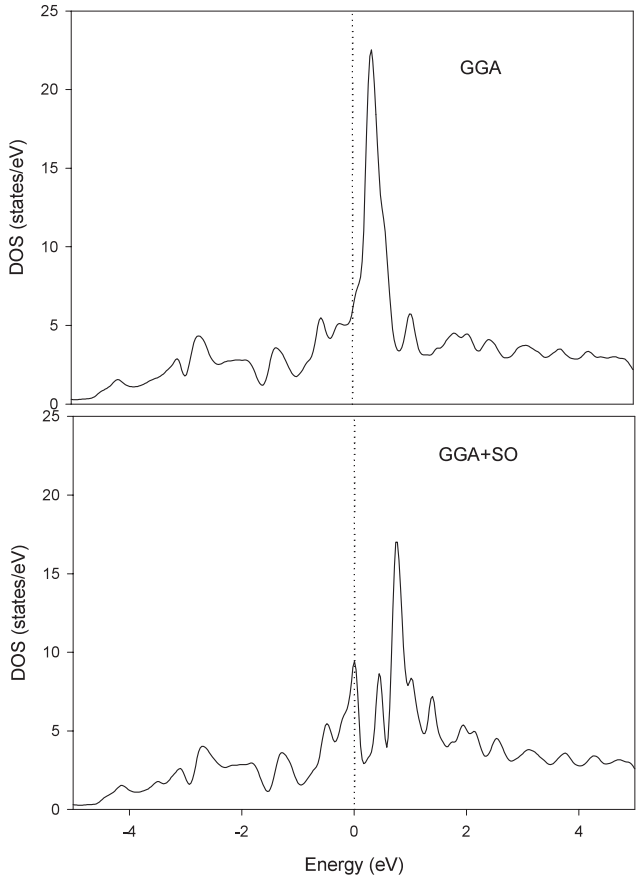

Figure 2. Total DOS of USn_3 in the presence and absence of SO.

values are of the same order of magnitude, but they are all about one order of magnitude smaller than the experimental value. This disagreement between theory and experiment has been attributed to electron–phonon interactions and to many body effects such as spin fluctuations in the system [15]. The connection between the calculated and experimental values of γ is written as

$$\gamma_{\mathrm{exp}} = \gamma_{\mathrm{band}}(1 + \lambda)$$

where λ is an enhancement factor taking electron–phonon interaction and many body effects into account. The calculated values for λ in different approaches are also given in table 2.

The total DOS of USn_3 near the Fermi energy in the presence and in the absence of SO are shown in figure 2. It is clear that the larger value of γ obtained with the SO is due to the existence of a peak at E_{f} in the DOS curve. In this case the total DOS of USn_3 is split into two disconnected parts. These two peaks correspond to the $j = \frac{5}{2}$ and $j = \frac{7}{2}$ 5f shell bands on the uranium site. The peak corresponding to the $j = \frac{5}{2}$ 5f band is located exactly at E_{f}, and this is the reason for the enhancement of the total DOS at the Fermi level in the presence of the SO. It should be noticed that Eriksson *et al* [16] have also shown that the full relativistic corrections increase the DOS at E_{f} for USn_3. The value of γ found using LDA (or LDA + SO) is larger than the corresponding value obtained by using GGA (or GGA + SO). This is probably due to the fact that the LDA overestimates the extent of localized orbitals, thereby increasing $D(E_{\mathrm{f}})$.

The band structure of USn_3 has been previously calculated [4] using a relativistic version of the augmented spherical wave method. Here in order to work out the effect of spin–orbit interaction on the electronic properties of system we have also calculated the electronic band structure both in the absence and in the presence of the SO (figure 3). While there is a good agreement between our result in the presence of the SO and the previous one, we can infer the following points from the comparison between the results in the presence of SO and those in the absence of SO.

(i) The SO coupling removes the spin degeneracy in the electronic band structure and hence the energy band is split into two subbands. This is in agreement with Moroz *et al* [17] for the case of quasi-one-dimensional systems.
(ii) The above-mentioned splitting occurs more dramatically in energy levels that are close to the Fermi energy and is greater in the region between Γ and X, R and M points in the first BZ.
(iii) As a result of the splitting in the energy band, two different types of charge carriers, with different effective masses, both in the range of heavy fermions, are involved.
(iv) The flatness in some parts of the energy bands below the Fermi energy around the points X and Γ in the first BZ indicates that there are some charge carriers with large effective masses.

To further understand the role of SO coupling and $p_{1/2}$ orbitals in the electronic properties we have calculated the total and partial density of states (DOS) by the tetrahedron method [18]. The total DOS for U and Sn atoms are shown in figure 4. The DOS at the Fermi level is dominated by 5f partial contributions, which prove their dominance in the transport properties of USn_3. It is observed that in the presence of SO coupling, the partial DOS of U 6p orbitals is split (by 7.23 eV) into two disconnected parts corresponding to $6p_{1/2}$ and $6p_{3/2}$ and the addition of $p_{1/2}$ local orbitals makes this splitting even larger (7.53 eV). The calculated spin–orbit splitting for the 5f states is 0.79 eV, which is not far from 1.1 eV obtained from a fully relativistic calculation for the 5f atomic orbitals [16]. Considering the large atomic number of U compared to Sn, the SO effect is expected to be more dramatic in uranium than in tin. Our results, as shown in figure 4, confirm this expectation. As the SO splitting in the DOS is only 1.04 eV which is due to Sn 4d states. We ignored the SO effect for Sn and only considered it for U in calculating the EFG.

3.2. Effect of pressure on electric field gradient

Any nucleus with a nuclear spin quantum number $I \geqslant 1$ has a nonspherical nuclear charge distribution and an electric quadrupole moment Q. The nuclear quadrupole interaction can be used to probe the electronic charge distribution surrounding such a nuclear site.

The interaction between the quadrupole moment Q and the electric field gradient (EFG) at the atomic site can be measured by various methods and is used for the characterization of surfaces, impurities and vacancies [19, 20]. Blaha *et al* [21, 22] developed an efficient method for calculating the EFG, in which the EFG can be derived directly from the general potential upon which the band calculation is based without the need for any additional Sternheimer factors. Using this method of calculation (within GGA) we investigated the effect of pressure on the EFG in USn_3 both in the presence and in the absence of spin–orbit interaction. Figure 5 shows the EFG at the Sn site plotted as a function of unit cell volume. It is seen that this EFG increases with the pressure. da Jornada *et al* [23] have observed a similar behaviour for sp element metals. The spin–orbit interaction reduces the calculated EFG by a small amount that is rather independent of the unit cell volume. The calculated EFG at the Sn site are given in

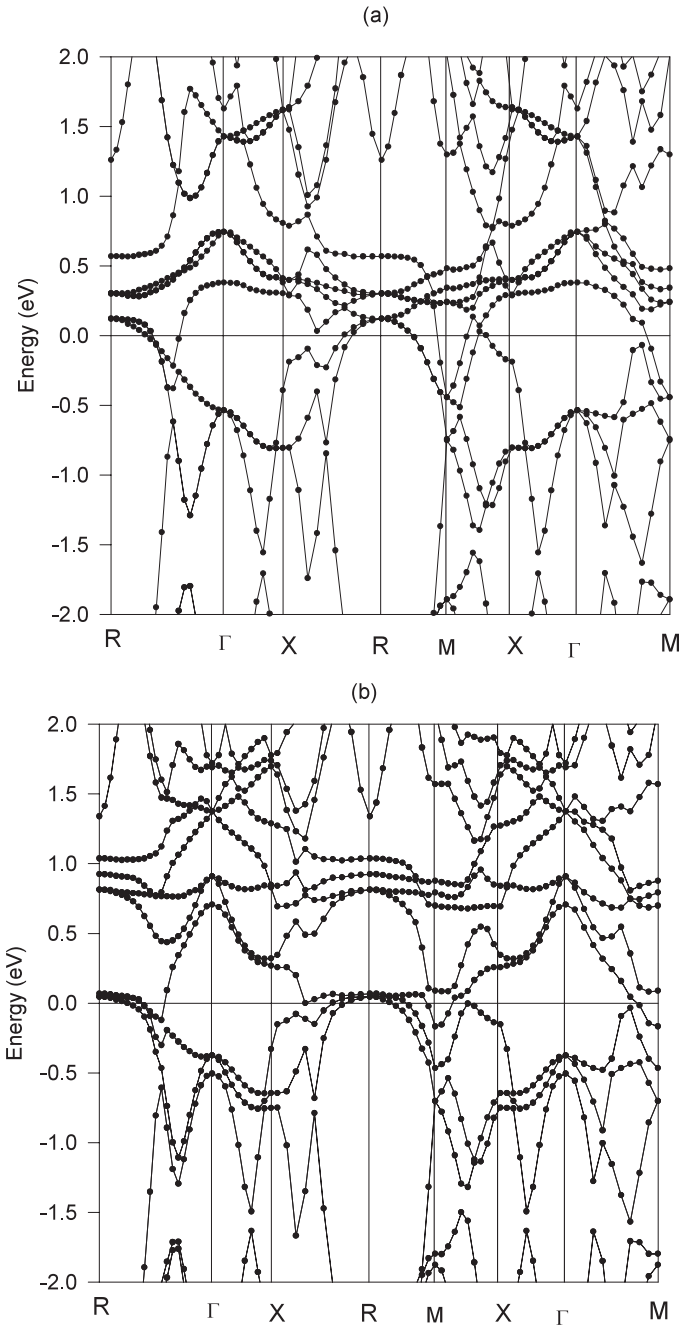

Figure 3. Band structure of USn_3 at the equilibrium lattice parameter (a) in the absence of the SO term and (b) in the presence of the SO term. The amount of spin–orbit splitting is different along different symmetry directions, being the greatest at the point M in the first BZ.

table 2. To our knowledge no experimental EFG values for USn_3 are available. It is clearly seen that the results obtained within LDA and GGA are similar, and in both approximations spin–orbit interaction decreases the value of the EFG by a small amount. The non-significant

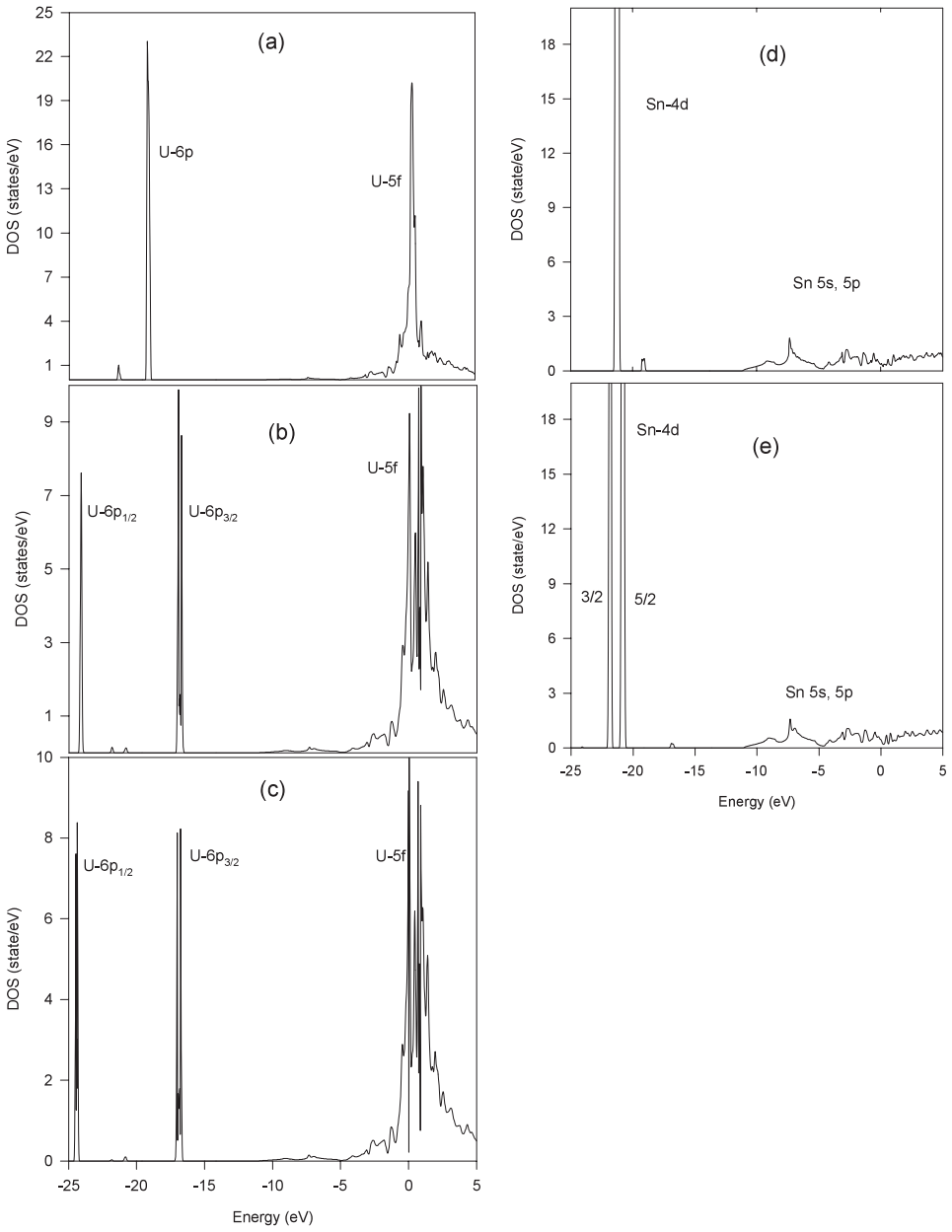

Figure 4. Total DOS of the U atom ((a) in the absence of spin–orbit coupling, (b) in the presence of spin–orbit coupling and (c) in the presence of spin–orbit coupling using a $p_{1/2}$ local orbital) and total DOS of the Sn atom ((d) in the absence of spin–orbit coupling and (e) in the presence of spin–orbit coupling).

effect of the spin–orbit interaction on the EFG has also been observed by Divis *et al* [24] in $GdNi_2B_2C$ compound.

The main contribution to the EFG originates from the anisotropy of the charge distribution close to the nuclei. These contributions can be further decomposed according to different

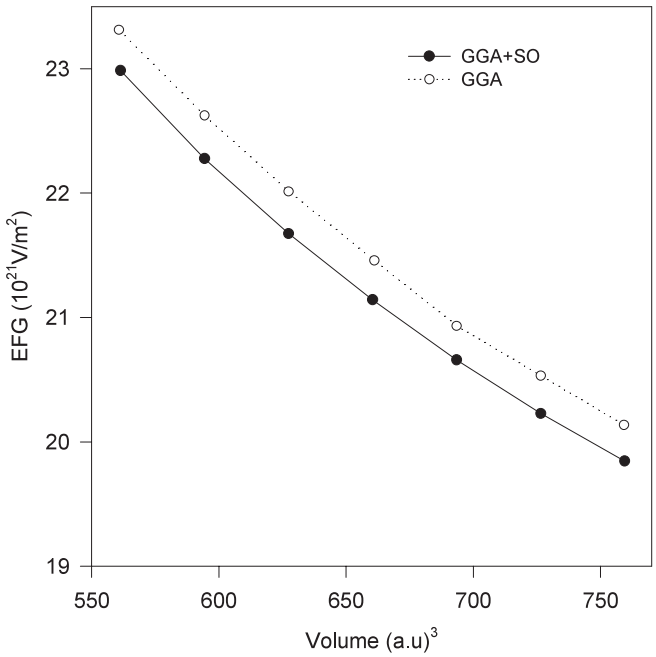

Figure 5. EFG at the Sn site as a function of unit cell volume.

combinations of wavefunctions, namely into s–d, p–p and d–d terms [22]. We have calculated these terms at the Sn site as a function of volume (figure 6). It is seen that the s–d contribution is negligible whereas the p–p one is dominant. A similar situation has been observed for sp metals and also for 3d and 4d transition metals [22]. Additionally we found that the p–p and d–d contributions to the EFG have opposite signs. (Note that the asymmetry parameter is zero for this point group.)

A measure for the nonspherical charge distribution based on p and d charges (Δn_{p}, Δn_{d}) inside the muffin-tin sphere can be written as [22]

$$\Delta n_{\mathrm{p}} = \tfrac{1}{2}(n_{\mathrm{p}_x} + n_{\mathrm{p}_y}) - n_{\mathrm{p}_z}$$
$$\Delta n_{\mathrm{d}} = n_{\mathrm{d}_{xy}} + n_{\mathrm{d}_{x^2-y^2}} - n_{\mathrm{d}_{z^2}} - \tfrac{1}{2}(n_{\mathrm{d}_{xz}} + n_{\mathrm{d}_{yz}}).$$

We have calculated Δn_{p} and Δn_{d} at different volumes (pressures); the results are shown in figure 6. It can be clearly seen that the nonsphericity of the charge, for both p and d orbitals, is increased by applying pressure. The positive value of the Δn_{p} can be easily understood by inspection of the partial density of states. In figure 7(a) the P_z and $\frac{1}{2}(P_x + P_y)$ of Sn are presented. We notice the dominance of the $\frac{1}{2}(P_x + P_y)$ below the Fermi energy, that leads to the positive value of Δn_{p}. The reason for increasing EFG with pressure can also easily be understood by inspection of the partial DOS. We calculated the difference $\frac{1}{2}(P_x + P_y) - P_z$ over a wide pressure range and show two pressure examples in figure 7(b). Since the dominant part of nonsphericity in the charge distribution is increasing with pressure, the resultant Sn EFG increases with pressure too.

Considering the fact that the 4d shell of Sn is completely full and consequently should be spherically symmetric, we might expect Δn_{d} to be zero at this site. The small asymmetry from the d contribution probably results from the tails of the wavefunctions from other atomic spheres entering the Sn atomic sphere. A similar behaviour has been observed at the

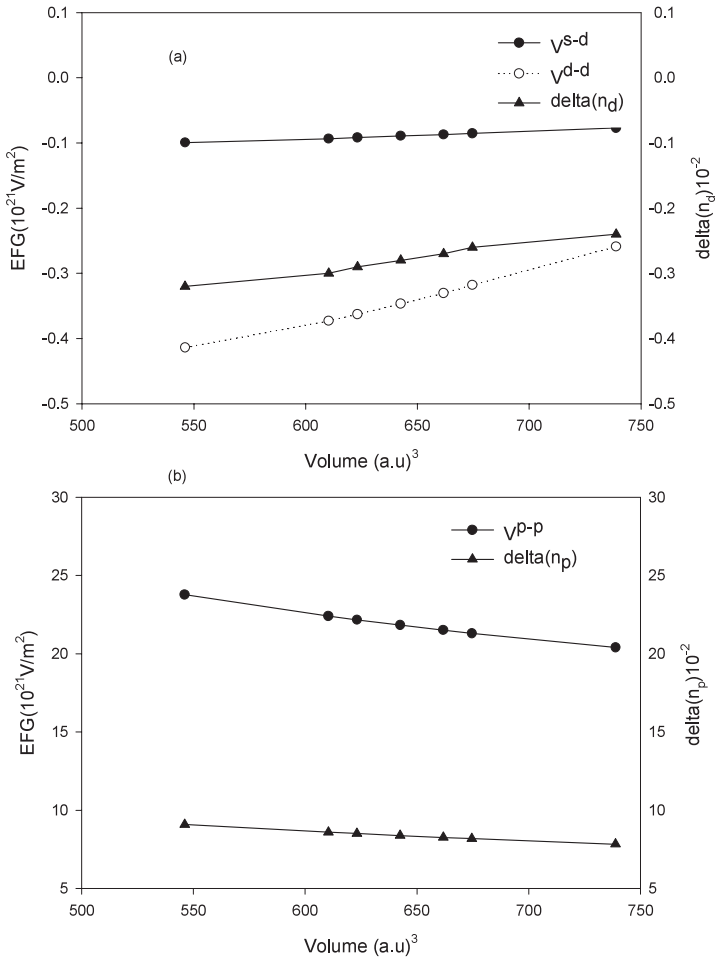

Figure 6. s–d, d–d and p–p contributions to the EFG at the Sn site and nonspherical charge of d and p orbitals as a function of unit cell volume.

In site of $CeIn_3$ [25]. The negative values of Δn_d inside the Sn muffin-tin sphere can then be interpreted as originating from the U 6d orbital tails entering inside this sphere. To understand such behaviour more clearly we have compared the e_g (t_{2g}) partial DOS of U 6d with the $5d_{x^2-y^2}$ ($5(d_{xy} + d_{yz})$) partial DOS of Sn 5d orbitals in figure 8. There is some small Sn $5d_{x^2-y^2}$ ($5(d_{xy} + d_{yz})$) contribution to the DOS in the energy range above -8 eV, which shows an energy dependence with similar features to that of e_g (t_{2g}) for U 6d states. Apparently these states are the tails of U 6d (t_{2g} and e_g) states and arise from wavefunctions centred at U but reaching inside the Sn atomic spheres.

4. Conclusions

We have found that the inclusion of spin–orbit interaction in U improves the results obtained for USn_3, but the addition of $p_{1/2}$ local orbitals does not introduce any very considerable change in the results. The amount of spin–orbit splitting in the density of states found for uranium orbitals is more than that for tin, which is to be expected because of the heavier uranium.

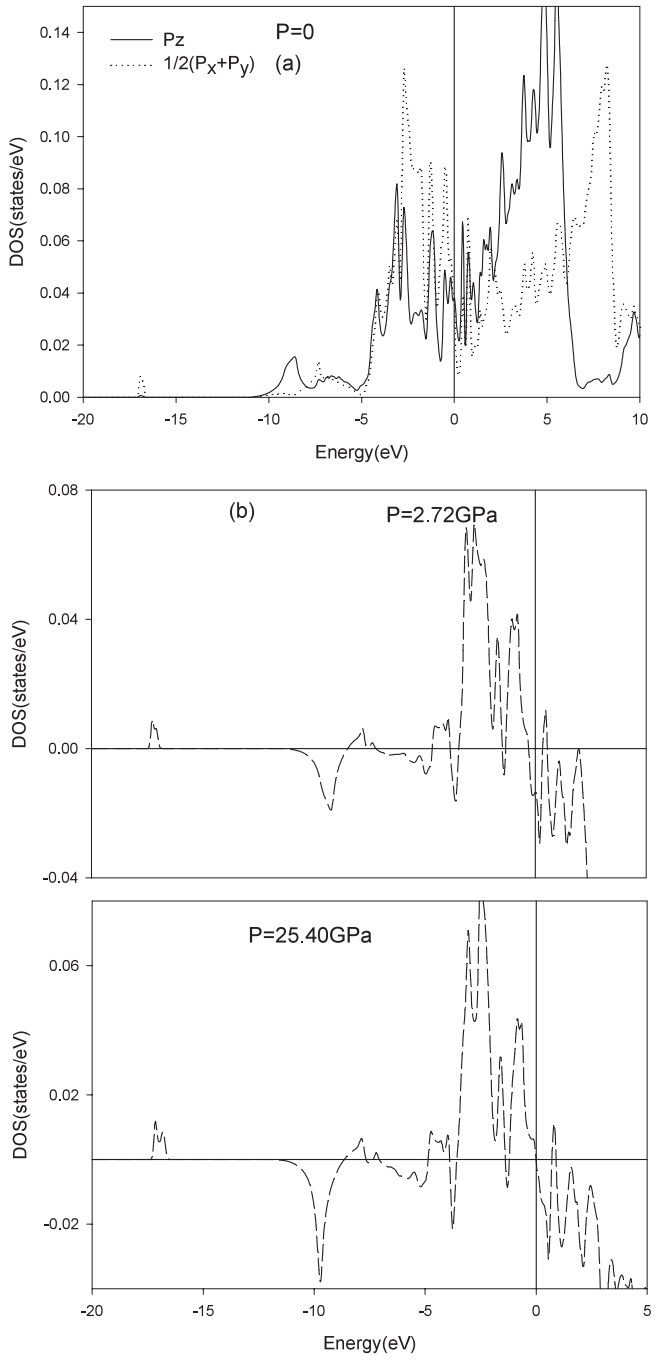

Figure 7. (a) Partial DOS curves at zero pressure, (b) the contribution of $\frac{1}{2}(P_x + P_y) - P_z$ in the DOS at two different pressures.

Furthermore we have shown that the EFG is zero at the U site, and has a large value at the Sn site. The large value is due to the anisotropy in the charge distribution close to the Sn nuclei

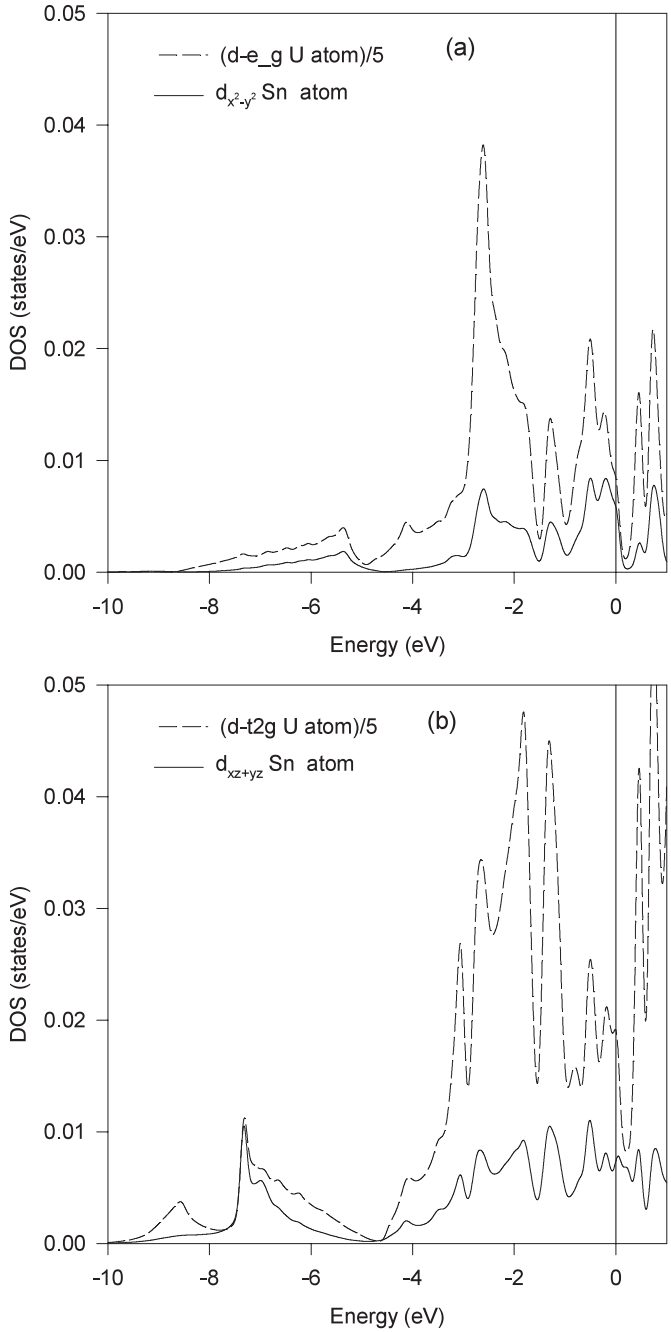

Figure 8. (a) Partial DOS of e_g U 6d states and Sn $5d_{x^2-y^2}$ states, (b) partial DOS of t_{2g} U 6d states and Sn $5(d_{xy} + d_{yz})$ states.

originating from p–p contributions. The EFG at the Sn site increases with pressure. The inclusion of spin–orbit interaction decreases the EFG by a small amount that is independent of pressure.

Acknowledgments

The authors would like to acknowledge the fruitful discussions with and also computational assistance of S Jalali Asadabadi and M Jamal.

References

[1] Hasegawa A 1985 *J. Magn. Magn. Mater.* **52** 425
[2] Scheidt E-W, Fraunberger G, Rieger J J, Mielke A, Kim W W and Stewart G R 1995 *J. Alloys Compounds* **218** 5
[3] Loewenhaupt M and Loong C-K 1990 *Phys. Rev.* B **41** 9294
[4] Cornelius A L, Arko A J, Sarrao J L, Thompson J D, Hundley M F, Booth C H, Harrison N and Oppeneer P M 1999 *Phys. Rev.* B **59** 14473
[5] Norman M R, Bader S D and Kierstead H A 1986 *Phys. Rev.* B **33** 8035
[6] Blaha P, Schwarz K, Madsen G K H, Kvasnicka D and Luitz J 2001 *WIEN2K, 'An Augmented Plane Waves + Local Orbitals Program for Calculating Crystal Properties'* Karlheinz Schwarz, Techn. Universitat Wien, Austria, ISBN 3-9501031-1-2
[7] Perdew J P, Burke S and Ernzerhof M 1996 *Phys. Rev. Lett.* **77** 3865
[8] Singh D J 1994 *Planewaves, Pseudopotentials and the LAPW Method* (Dordrecht: Kluwer–Academic)
[9] Kunes J, Novak P, Divis M and Oppeneer P M 2001 *Phys. Rev.* B **63** 205111
[10] Nordstrom L, Wills J M, Andersson P H, Soderlind P and Eriksson O 2001 *Phys. Rev.* B **63** 035103
[11] Kunes J, Novak P, Schmid R, Blaha P and Schwarz K 2001 *Phys. Rev.* B **64** 153102
[12] Palenzona A and Manfinetti P 1995 *J. Alloys Compounds* **221** 157
[13] Murnaghan F D 1944 *Proc. Natl Acad. Sci. USA* **30** 244
[14] Meresse Y, Heathman S, Le Bihan T, Rebizant J and Brooks M S S 1999 *J. Alloys Compounds* **284** 27
[15] Strange P 1986 *J. Phys. F: Met. Phys.* **16** 1515
[16] Eriksson O, Brooks M S S and Johansson B 1989 *Phys. Rev.* B **39** 13115
[17] Moroz A V and Barnes C H W 1999 *Phys. Rev.* B **60** 14272
[18] Blochl P E, Jepsen O and Andersen O K 1994 *Phys. Rev.* B **49** 16223
[19] Wichert Th and Recknagel E 1986 *Topics in Current Physics* vol 40, ed U Gonser (Berlin: Springer)
[20] Klas T, Voigt J, Keppner W, Wesche R and Schatz G 1986 *Phys. Rev. Lett.* **57** 1068
[21] Blaha P, Schwarz K and Dederichs P H 1988 *Phys. Rev.* B **37** 2792
[22] Blaha P, Schwarz K and Herzig P 1985 *Phys. Rev. Lett.* **54** 1192
[23] da Jornada J A H and Zawislak F C 1979 *Phys. Rev.* B **20** 2617
[24] Divis M, Schwarz K, Blaha P, Hilscher G, Michor H and Khmelevskyi S 2000 *Phys. Rev.* B **62** 6774
[25] Lalic M V, Mestnik-Filho J, Carbonari A W, Saxena R N and Haas H 2002 *Phys. Rev.* B **65** 054405